Impact of the Relative Humidity on the Performance Stability of Anion Exchange Membrane Fuel Cells Studied by Ion Chromatography

Julian Lorenz,[a,‡,*] *Holger Janßen,*[b,c,‡] *Karam Yassin,*[d] *Janine Leppin,*[b] *Young-Woo Choi,*[e] *Jung-Eun Cha,*[e] *Michael Wark,*[c] *Simon Brandon,*[d,f] *Dario R. Dekel,*[d,f] *Corinna Harms,*[a] *Alexander Dyck*[b]

[a] German Aerospace Center (DLR), Institute of Engineering Thermodynamics, Carl-von-Ossietzky-Str. 15, 26129 Oldenburg, Germany

[b] German Aerospace Center (DLR), Institute of Networked Energy Systems, Carl-von-Ossietzky-Str. 15, 26129 Oldenburg, Germany

[c] Carl von Ossietzky University, Institute of Chemistry, Carl-von-Ossietzky-Str. 9-11, 26129 Oldenburg, Germany

[d] The Wolfson Department of Chemical Engineering, Technion – Israel Institute of Technology, Haifa 3200003, Israel

[e] Fuel Cell Research & Demonstration Center, Korea Institute of Energy Research (KIER), 20-41 Sinjaesaengeneogi-ro, Haseo-myeon, Buan-gun, Jeollabuk-do 56332, Republic of Korea

[f] The Nancy & Stephen Grand Technion Energy Program (GTEP), Technion – Israel Institute of Technology, Haifa 3200003, Israel

* E-mail: julian.lorenz@dlr.de, Phone: +49-441-99906-323

‡ J.Lo. and H.J. contributed equally to this work.

KEYWORDS.
Degradation Products, AEMFC, Nucleophilic Substitution, Longevity, Quaternary Ammonium Ions

ABSTRACT.

Although substantial improvement of the performance of anion exchange membrane fuel cells (AEMFC) was achieved, longevity is still the main challenge for AEMFC technology which is attributed to the degradation of the functional groups of applied membranes and ionomers. Contrary to *ex-situ* material stability studies, we demonstrate here the application of ion chromatography to quantify the amounts of degradation products in the exhaust water during different fuel cell operation conditions on the example of trimethylbenzyl ammonium as a functional group. Higher amounts of degradation products were detected directly after equilibration and completion of polarization curves compared to performance stability measurements under constant load. Moreover, the performance stability dependent on the relative humidity of the anode and cathode feed gases was evaluated. Elevated losses of ionic groups were observed in the anode exhaust water at high humidity fuel cell operation, although higher degradation rates were determined for the cathode side by modeling the performance stability. In contrast, higher amounts of degradation products were detected in the cathode exhaust water under low humidity conditions. However, the mobility of water and degradation products under different fuel cell operation conditions impede a detailed allocation of observed degradation to one electrode. The demonstrated combination of *in-situ* electrochemical measurements, corresponding *ex-situ* degradation measurements and modeling data gives comprehensive insights into the evaluation of the performance stability of anion exchange membrane materials under fuel cell operation, which could exceed *ex-situ* durability experiments based on the membrane materials itself.

1. Introduction

The anion exchange membrane fuel cell (AEMFC) attracted increasing attention due to the development of new hydroxide conducting polymer materials which enabled competition regarding begin of life performance with its acidic counterpart, the proton exchange membrane fuel cell (PEMFC).[1-4] The potential use of non-platinum group metals as catalysts[5-7] and the opportunity to use non-fluorinated membranes[8-9] are seen as essential cost advantages compared to PEMFC. However, the limited long-term performance stability is the main hurdle for the commercialization of AEMFC technology.[3, 10-12] The instability is mostly attributed to the degradation of the polymers functional group during operation, which serves as anion (hydroxide) conducting functionality.[3, 10] Thus, the overall performance of the AEMFC decays with ongoing degradation of the anion exchange membrane (AEM) and the anion exchange ionomer (AEI) in the catalyst layers.

Several anion-conducting groups are discussed in the literature for AEMFC application. Besides the evaluation of fundamental properties like the ion exchange capacity (IEC), water uptake, and ion conductivity, the study of the stability of polymer backbones and anion conducting groups is another strong focus.[10, 13-15] Quaternary ammonium (QA) groups like triethylbenzyl ammonium (TEBA) and trimethylbenzyl ammonium (TMBA) are most commonly used.[10, 16] The degradation processes mainly proceed chemically by a Hofmann elimination at the β-hydrogens (Scheme 1a) and the nucleophilic substitution of the QA by an attack of the hydroxide ion at the α-carbon atom (Scheme 1b).[10, 13] Because Hofmann elimination cannot take place at TMBA this QA is considered as more stable.[13, 16] Demethylation of TMBA (Scheme 1c) might also take place but was described as a minor degradation route.[16] The stability of the TMBA group can be improved by the addition of acyl spacers between the QA and the polymer backbone which prevents nucleophilic

substitution, but the improved stability has not been confirmed under AEMFC operating conditions.[12, 17]

The stability of functional groups themselves or their binding to a polymer backbone are usually studied *ex-situ* by immersing them into concentrated hydroxide solution (e.g., 1-10 M KOH) at a defined temperature and duration.[13-15, 18] Evaluation of either the ion conductivity and IEC or the loss of QA by NMR and UV/Vis spectroscopy reveals the occurring degradation.[13, 19-20] However, these *ex-situ* tests do not resemble the true stability of AEM during operation because the hydroxide is solvated by water molecules decreasing its nucleophilic strength.[15, 21]

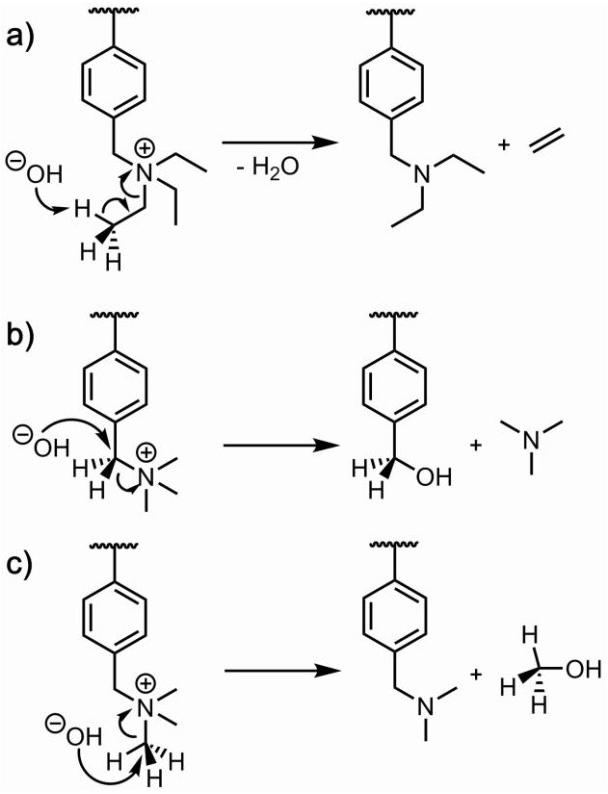

Scheme 1. Main degradation pathways of QA functional groups by a) Hofmann elimination at triethylbenzyl ammonium ions (TEBA), b) nucleophilic substitution at trimethylbenzyl ammonium (TMBA), and c) demethylation of TMBA.

Recently, a new methodology was introduced in which the amount of water per hydroxide molecule, defined as hydration level λ, can be controlled.[21] It was demonstrated that degradation becomes drastically faster at low hydration levels of $\lambda < 4$, which are likely to occur at high current densities during fuel cell operation and especially at the cathode where water is consumed during the oxygen reduction reaction.[15, 21] The methodology was initially described for small molecules (different QA groups), but subsequently applied to poly(phenylene oxide) (PPO) based polymer backbones functionalized with TMBA and TEBA as AEI.[22] This study showed a further acceleration of the degradation process, which was explained by an increase of hydroxide reactivity due to the lower polarity of the polymer environment. These experiments were further supported by simulation studies[23-24] showing the development of low hydration levels during operation and highlight the crucial role of water management for the longevity in AEMFC. However, experimental evaluation of existent hydration levels during AEMFC operation is challenging. A quartz crystal microbalance study, which allows determining the mass change due to the uptake of water from a humidified gas phase, suggests a hydration level of $\lambda \approx 4$ and between 6 and 10 at a relative humidity (RH) level of roughly 30% and 60%, respectively, depending on the thickness of the casted film of Tokuyama AS-4 AEI.[25]

In another degradation study, a thermogravimetric method was used to evaluate the stability of an AEM based on PPO functionalized with trimethyl-pentyl-ammonium as QA by measuring the change of its IEC dependent on the RH and temperature to mimic fuel cells operation conditions.[26] A hydration level of $\lambda \approx 5$ and $\lambda \approx 4$ were determined for RH values of 65% and 50% at 60°C, respectively. Degradation studies at an RH value of 50% (with intervals at 65%) showed a decrease of the IEC from rough 1.6 to 1.4 mmol g^{-1} after 180 h.[26] Also, the deviation between the membrane degradation at 50% RH and 100°C ($\lambda \approx 3$) was shown compared to *ex-situ* studies in 1 M NaOH

(less degradation) and 10 M KOH (more drastic degradation) electrolytes. Furthermore, a different degradation mechanism was reported for *in-situ* AEMFC testing compared to *ex-situ* methods for a PPO-TMBA AEM as well as for QAs with different structured side chains.[17] These studies demonstrate the discrepancy between stability evaluation solely from *ex-situ* measurements and highlighting the requirement of studies mimicking realistic conditions or measuring in-situ AEMFC performance stability.

Performance stability evaluation under AEMFC operation with the AEM and the AEI incorporated in membrane electrode assemblies (MEA) are typically performed at constant current densities (e.g., 100 mA cm^{-2}) and cell temperatures between 40 and 80 °C with varying RH of feed gases and further operation conditions.[3, 12] These conditions allow constant consumption and generation of water and are therefore intending to study the stability dependent on water management and reaction transport. Also, evaluations under constant voltage mode are performed to study specific degradation processes dependent on the potential.[12] For constant current density mode, the potential decay is measured over time and, in general, fast performance losses after 100 to 200 h demonstrate the challenge of AEMFC longevity, and only a few studies have demonstrated MEAs lasting for 600 to 800 h with degradation rates of 0.2 to 0.5 mV h^{-1}.[3, 27-29] Only recently, lifetimes above >1000 h were demonstrated.[30-31]

The determination of the AEM and AEI stability based on evaluations at MEA level is challenging because different degradation processes could happen in parallel and are dependent on varying fuel cell operations. The AEM might degrade by chemical degradation of the polymer backbone and QA functionality (Scheme 1), but also mechanical failure might occur.[12] For AEI degradation, differentiation between the anode and cathode electrode is necessary.[12] At the cathode, electrochemical oxidation of the AEI (e.g., oxidation of the phenyl group[32]) must be

considered as well as chemical degradation due to rather low hydration levels at high current densities.[15] The AEI on the anode side can chemically degrade by adsorption of ammonium groups at the catalyst surface that lead to cationic group degradation, which was described to be lower on PtRu anode catalysts[33], but also physical aging of the AEI might occur.[12] Allocation of a degradation process to an observed phenomenon in fuel cell testing is thus demanding. Furthermore, but not discussed here, the electrocatalyst is also prone to degradation effects.

In this study, the performance stability of MEAs is investigated under different fuel cell operating conditions. The decay in performance is related to the degradation of the AEM and AEI by application of ion chromatography (IC) which allows the evaluation of degradation products in the exhaust water of the cathode and anode. While most studies solely rely on the performance or impedance data of the MEA to evaluate the membrane stability, IC analysis gives additional insight into specific degradation pathways dependent on the applied parameters. Moreover, sampling at different defined times in the course of the measurement allows stability evaluation under varying fuel cell operating conditions. Trimethylamine (TMA) is anticipated as the main degradation product of TMBA by nucleophilic substitution (Scheme 1b) but also its derivatives are investigated. Furthermore, the performance stability is evaluated dependent on the applied RH of the feed gas at the anode and cathode. Synthetic air instead of oxygen is used at the cathode to approach application-related conditions. Reduced RH values lead to low hydration levels determined by AEMFC modeling, which increases the nucleophilicity of the hydroxide ions and thus provoke a stronger degradation during MEA operation.[15, 23] The IC analysis complements the performance data and results in a more comprehensive understanding of the stability of the AEM and AEI materials.

2. Experimental

Materials. As AEM material quaternized poly(vinylbenzyl) trimethylammonium cross-linked with *N,N'*-bis(acryloyl)piperazine was used, and its synthesis is described elsewhere.[34] In short, a porous polyolefin substrate was impregnated with specific amounts of TMBA chloride and *N,N'*-bis(acryloyl)piperazine and polymerization was achieved by UV irradiation. Amounts of the QA and cross-linking agent were optimized to result in membranes with a uniform thickness of 23.4 µm and an IEC of 1.55 mmol g^{-1}.[34] The hydroxide conductivity was 40 mS cm^{-1} at 20 °C. The stability was evaluated *ex-situ* in 5 M KOH solution at 80 °C, and quite stable IEC and ion conductivity values for over 1500 h were demonstrated.[34] This improved stability was attributed to the high amount of QA in the narrow channels.[34]

Preparation of membrane electrode assemblies. MEAs were prepared by coating the membranes (25 cm^2) with a commercial Pt/C catalyst (HiSPEC® 4000, 40wt% Pt on Vulcan XC72R, Johnson Matthey) at the anode and cathode side using an automatic ultrasonic spray coating device (ExactaCoat FC, Sonotek) with a target loading of 0.5 mg_{Pt} cm^{-2} per electrode. AS-5 by Tokuyama Corp. was used as AEI with a weight loading of about 25wt% in the catalyst layer. An IEC value of 1.0 mmol g^{-1} for AS-5 was used for IC analysis as reported in the literature.[35] A PTFE-treated gas diffusion layer equipped with a microporous layer (Freudenberg H2315 I2C6) was used to assemble the MEA.

Fuel cell testing. The test bench G100 by Greenlight Innovation was used to study the MEAs. All experiments were done with hydrogen at the anode and CO_2-free synthetic air at the cathode with a stoichiometry of 6/10 (A/C) and a backpressure of 100 kPa at a cell temperature of 60 °C. The MEA was equilibrated by potentiostatic hold at 0.55 V, including a short potentiostatic step at 0.1 V for 15 min to remove remaining carbonate ions.[36] The performance of the MEA was

evaluated by performing polarization curves in galvanostatic mode in 0.2 A intervals. Afterwards, the study of the performance stability was started at a controlled current density to achieve an initial cell voltage of around 0.6 V. With decreasing cell voltage, the current density was lowered to keep the cell voltage between 0.6 and 0.4 V and to avoid fast irreversible degradation of the cell. The impact of the hydration level on the fuel cell operation (equilibration, polarization curve and performance stability) was studied by systematic variation of the RH of the feed gases. The chosen RH values were kept constant from beginning to end of the respective measurement. First, the performance stability was evaluated at 95% RH for both electrodes (95/95), and then the RH of feed gases was lowered separately to 60% at the anode (60/95) and at the cathode (95/60) and also coincidentally at both electrodes (60/60).

To evaluate the stability of the AEM and AEI materials, the exhaust water of the anode and cathode was analyzed for possible degradation products. Cooling traps made of stainless steel were installed behind the anode and cathode outlet of the measuring cell to collect the exhaust water of both electrodes separately. The cooling traps were held at room temperature and cleaned intensively between individual experiments. Condensation of reaction gases allowed collection of the degradation products in the exhaust water, which was immediately acidified and processed as described below by ion chromatography.

Ion chromatography. The device 850 Professional IC by Metrohm equipped with the column Metrosep C 4-100/4.0 (silica gel functionalized with carboxyl groups) was used to detect the degradation products from the AEM and ionomer in the exhaust water of the anode and cathode side. TMA and possible derivatives of TMA like dimethylamine (DMA) and monomethylamine (MMA) as well as ammonium (NH_4^+) were analyzed as shown by a study of Tokuyama Corp.[37] Water samples were acidified with 1 µL per mL sample volume of 2 mmol L^{-1} nitric acid and a

mixture of 1.7 mmol L^{-1} nitric acid and 0.7 mmol L^{-1} dipicolinic acid was used as eluent.[38] The flow rate of the eluent was 0.9 mL min^{-1} and a sample volume of 20 µL was injected for the analysis. Calibration curves for the specific compounds and calculation of the limit of quantification and limit of detection were performed and are provided in the supporting information (Figure S2).

Modeling. In order to further elucidate the effect of RH at anode and cathode on the performance stability of AEMFC, a one-dimensional isothermal and time-dependent model of AEMFCs operation was applied.[39] The computational domain includes a five-layer MEA consisting of an AEM, anode and cathode CLs, and anode and cathode gas GDLs. The model accounts for electrochemical reactions (ORR and HOR), mass transport across the MEA (gas transport through GDLs and CLs as well as liquid water), ion migration. Furthermore, the model calculates the chemical degradation kinetics of the ionomeric materials in the anode and cathode CLs and the membrane, whose local kinetics is set by the local water content. The model can predict the performance and performance stability of AEMFC (time-changes in IEC, represented by the hydroxide ions concentration).[23-24, 40]

The model is validated against experimental data for AEMFC operated with RH values of 95/95 at anode and cathode by tuning a single parameter for fitting the entire dataset, namely, the cathode electrochemical surface area. The remaining model parameters were derived from the experimental measurements. Then, for validating all other AEMFC performance curves, the only parameter to update was the RH values of the anode and cathode electrodes. The good agreement between the experimental and the predicted performance stability of AEMFCs shown in Figures S3 and S4 provides strong confidence in the model validity and robustness.

3. Results and Discussion

Automated ultrasonic spray coating enabled the production of reproducible MEAs with average catalyst loadings at the anode and cathode of 0.49 ± 0.03 mg_{Pt} cm^{-2} and 0.56 ± 0.06 mg_{Pt} cm^{-2}, respectively (Table S1). A uniform and reliable fabrication of MEAs is a prerequisite for the evaluation of different test parameters.[41] After equilibrating the MEAs, polarization curves were conducted to assess the performance of prepared samples. Although optimization of the cell performance dependent on the water management was out of scope of this study, polarization curves were recorded with varied RH values, which were also applied during the equilibration procedure and evaluation of the stability under galvanostatic operation conditions. The influence of the different applied RH at the anode and cathode feed gases on the performance is shown in Figure 1. The highest peak power density of 330 mW cm^{-2} was obtained at high RH values at the anode and cathode (95/95). With decreasing RH at the anode (60/95) a peak power density of 300 mW cm^{-2} was still achieved, indicating that water produced by the hydrogen oxidation reaction at the anode side might compensate for lower humidity at this electrode.[42] A lower performance of 256 mW cm^{-2} and 186 mW cm^{-2} was observed for RH values of 60/60 and 95/60, respectively. For the latter case, the noticeable lower power density might indicate a degradation during the equilibration procedure as will be discussed below. The humidity-dependent performance agrees well with reports in the literature where also better performances for higher RH values at either the cathode or both electrodes were shown.[43-44] The beneficial effect of the water management on the performance of AEMFC was also highlighted by Omasta and co-workers.[36, 42] These authors demonstrated that an optimized balance of water in the membrane and electrodes avoids both, dry-out events at the cathode and flooding of the anode. Thus, more stable operation behavior and a substantial performance increase were achieved.[36]

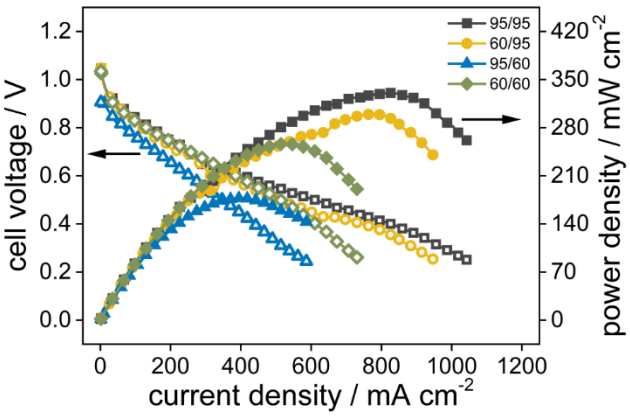

Figure 1. Impact of the relative humidity of the anode and cathode feed gases (A/C) on the cell voltage (open symbols) and the power density (solid symbols) of MEAs fed with hydrogen and synthetic air at the anode and cathode, respectively. The MEAs were operated at a constant stoichiometry of 6/10 (A/C), a backpressure of 100 kPa and a cell temperature of 60 °C. Catalyst loadings of the anode and cathode are given in Table S1.

The performance stability was studied in galvanostatic mode by applying a current density to achieve a resulting cell voltage of about 0.6 V. Thus, different current densities for different MEA samples were applied dependent on their performance. For high RH values at anode and cathode (95/95), the MEA was operated at 300 mA cm^{-2} and the behavior of the cell voltage over time is shown in Figure 2a. Small fluctuations in the cell voltage were observed during the equilibration procedure (up to ~16 h), which might originate from insufficient humidification of the membrane at the beginning of the measurement. The more stable behavior after running the polarization curve (~25 h) emphasizes an additional activation due to an enhanced water production at higher current densities during the measurement of the polarization curve in addition to the equilibration procedure at constant voltage.[45] After a total run time of 73 h the cell voltage dropped drastically. Possibly, the behavior can be explained by anode flooding during continuous fuel cell testing, which was described as reversible.[32] Also, mechanical failure of the membrane might occur and

interfacial delamination between the membrane and electrode could happen, but are unexpected after rather short testing times.[12]

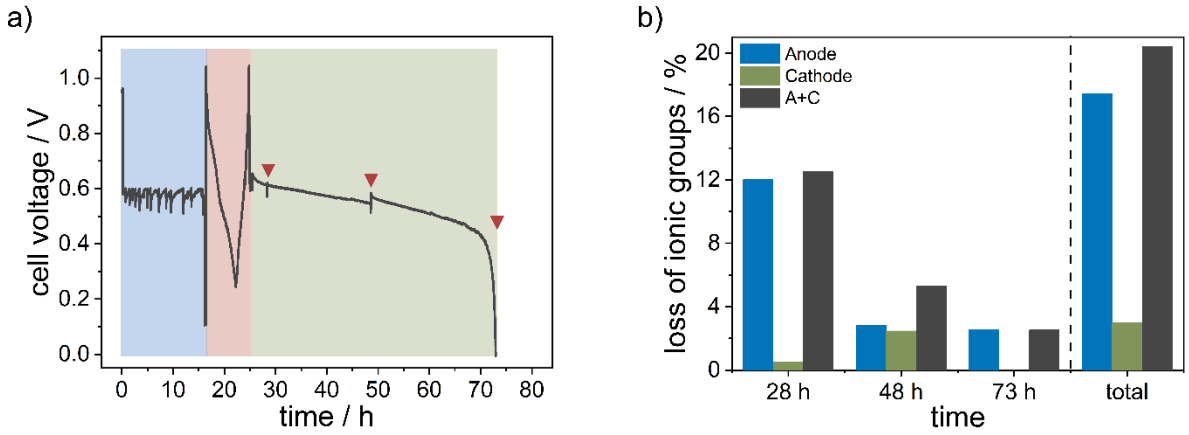

Figure 2. Performance stability of an MEA operated at high relative humidity at the anode and cathode (95/95). a) Performance behavior at different operation conditions (equilibration in blue, polarization curve in red and galvanostatic control in green) with an applied current density of 300 mA cm^{-2} during galvanostatic control. Triangles mark the points of sampling of exhaust water. b) Loss of ionic groups as the sum of TMA, DMA, MMA and NH_4^+ by quantification of degradation products in the anode and cathode exhaust water using ion chromatography.

The performance decay can be related to the loss of ionic groups of the AEM and AEI quantified by IC of the exhaust water of the anode and cathode (Figure 2b). As degradation product TMA was expected (Scheme 1b), but also its derivatives DMA and MMA as well as NH_4^+ were detected. The exact degradation mechanism resulting in the derivatives as well as the structure of AS-5 ionomer is rather unclear, but the same pattern of degradation products in IC data was reported by Tokuyama Corp.[37] Consequently, TMA, DMA, MMA and $NH4^+$ were considered here in the IC analysis. The mass concentration of degradation products calculated by integration of the peak areas obtained in the chromatogram (e.g., Figure S2) was transferred to the amount of substance n_{IC}. The sum of amounts of substances of degradation products (TMA, DMA, MMA and $NH4^+$)

was related to the present initial amount of QA considering the mass loading *m* of the AEM and AEI in the MEA and their IEC (Eq. 1). The present initial amount of QA is determined for the whole MEA, while IC analysis was related to degradation products determined in the anode and cathode exhaust water or as a sum of both.

$$\text{loss of ionic groups [\%]} = \frac{n_{\text{IC,anode}} + n_{\text{IC,cathode}}}{m_{\text{AEI}} \cdot \text{IEC}_{\text{AEI}} + m_{\text{AEM}} \cdot \text{IEC}_{\text{AEM}}} \quad (1)$$

Although applied parameters during fuel cell testing might result in higher degradation rates rather at one electrode compared to the other, a correlation of IC data with occurred degradation at the anode or cathode is hardly possible due to mobility of water and degradation products under different fuel cell operating conditions. Also, a separation of the degradation between AEM and AEI is not possible from the IC data due to possibly similar QAs of the AEM and AEI material.[42, 46 37] Thus, the analysis of IC data is based on the sum of AEM and AEI degradation and the nucleophilic substitution of TMBA is considered as main degradation pathway. Nevertheless, we separate the IC analysis in degradation products found in the exhaust water of the anode and the cathode because this might give additional insights into the AEMFC performance stability, but this does not necessarily mean that the degradation has taken place at the anode or cathode.

The highest amount of about 13% of degradation products was detected after 28 h. Minor amounts of 5 and 3% were detected after 48 and 73 h, respectively. In total, a loss of ionic groups of 20% was observed referring to the present initial amount of QA in the AEM and AEI. Thus, a great fraction of degradation is induced by the equilibration procedure and conducting of polarization curves. This might be explained by relatively long galvanostatic steps at higher current densities during the polarization curve. Under these conditions, low hydration numbers at the cathode are expected, which can result in a higher nucleophilicity of the hydroxide ions and subsequently to potentially higher degradation rates.[23, 47] Also, the potentiostatic hold at a low

value of 0.1 V during the equilibration procedure might be very harsh. The substantial degradation of the MEA at this state of operation could easily be overlooked because the longevity is usually analyzed by the performance decay and impedance data under galvanostatic control after the completion of polarization curves.[3] Also for PEMFC technology, implementation of MEA characterization by polarization curves and cyclic voltammetry during the long-term operation was described to induce additional degradation.[48] Consequently, experimental parameters of the equilibration procedure and polarization curves should be carefully chosen.

It is also noticeable that higher amounts of degradation products were found in the sample of the anode exhaust water at every time of sampling (Figure 2b). This might hint at ionomer degradation taking place at the anode, but also degradation products from the cathode and membrane can be transported to the anode. Complex water mobility during AEMFC operation and fluxes of ionic species between the electrodes hinders an allocation of observed degradation to one electrode.[15, 41] Thus, a higher fraction of observed degradation products in the anode exhaust water originate not necessarily from higher degradation rates at the anode. To understand the possible degradation process, the performance stability under applied conditions of high RH values at anode and cathode (95/95) was simulated. Figure 3 demonstrates λ and IEC profiles across the cell of AEMFC operated at 300 mA cm^{-2}. Low hydration levels of roughly $\lambda = 8$ were determined. The results at different times of operation show a reduction in the local IEC values in the cathode CL and in the membrane close to the cathode catalyst layer. This reduction indicates a degradation of the ionomeric materials, which is based on lower hydration levels at the cathode and causes performance decay over time, as previously discussed.[23-24, 40, 49-50] Thus, cathode ionomer and membrane degradation might be the reason for observed degradation products in the IC analysis. Back diffusion of water from the anode to cathode might compensate for low hydration levels at

the cathode, but even for high water diffusivity values, lower hydration levels were observed at the cathode.[24, 30-31, 51] Change of the anode catalyst to a PtRu material as done in recent AEMFC studies might improve the water level at the cathode due to enhanced kinetics of the hydrogen oxidation reaction and thus produce more water that can diffuse to the cathode.[12, 36] Also, the volumes of sampled exhaust water differ between the anode and the cathode side (Tables S3-S6). Higher volumes at the cathode side can be explained by the higher stoichiometry of the gas feed at this electrode, although water is consumed during the oxygen reduction reaction.

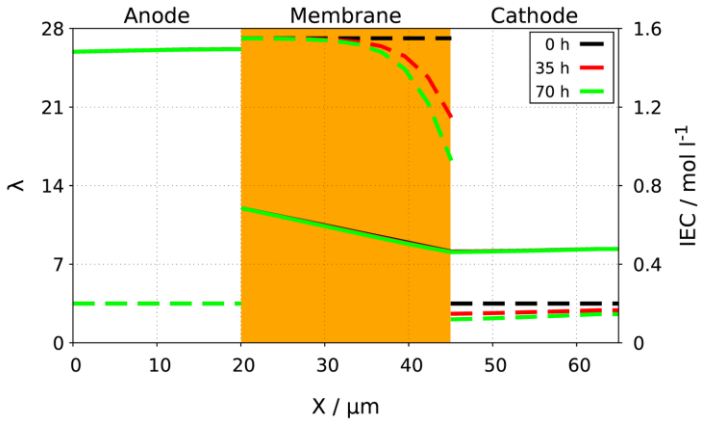

Figure 3. Modeling of hydration number (solid lines) and IEC (dashed lines) profiles, at different operation times, across the MEA of AEMFC operated at a constant current density of 0.3 A cm^{-2}, at high relative humidity at the anode and cathode (95/95).

The impact of the water content on different fuel cell operations was evaluated by varying the RH values of the anode and cathode feed gases. For individual MEA samples, the RH was lowered separately to 60% at the anode (60/95) and cathode (95/60), respectively, and then at both electrodes (60/60). The lower RH values resulted in different hydration levels across the cell determined by modeling (Figure S5). The reduced humidity at the cathode resulted in a decrease from $\lambda = 8$ to 4. At the anode the hydration level decreased from $\lambda = 26$ to 19 and 8 for RH values of (95/60), (60/95) and (60/60), respectively. The RH values were already applied during the

equilibration procedure, and the recording of polarization curves and their impact on the performance were discussed above. Current densities of 300 mA cm^{-2} (60/95), 216 mA cm^{-2} (95/60), and 336 mA cm^{-2} (60/60) were applied to achieve an initial cell voltage of 0.6 V for the evaluation of the RH impact on the performance stability. The lower current density for reduced RH at the cathode (95/60) indicates a degradation of the MEA before studying the performance stability, which can also be seen from the comparably low performance of this MEA in the polarization curve (Figure 1). Thus, premature degradation occurred possibly due to the low hydration levels. In contrast, a relatively high current density was applied in the case of the MEA at RH values of 60/60 despite the low humidification. In the course of the measurement the current densities were lowered to keep the cell voltage between 0.6 and 0.4 V.

Figure 4 shows the MEA operation dependent on the varied RH values. For lower humidity, at the anode, a similar behavior was observed compared to the high RH (95/95). The current density was steadily decreased after 44 h resulting in a smooth voltage decay. In case of reduced humidity at the cathode (95/60) a stronger decrease of the cell voltage was observed after the polarization curve, indicating a higher degradation rate possibly based on a reduced hydration level and thus more nucleophilic hydroxide ions (Figure 4b).[15] For the experiment at low RH at both electrodes, quite unstable behavior was observed during the equilibration of the cell, which likely originates from insufficient water management under these conditions. Also, the performance decreased relatively fast due to higher degradation rates at low humidity conditions (Figure 4c).

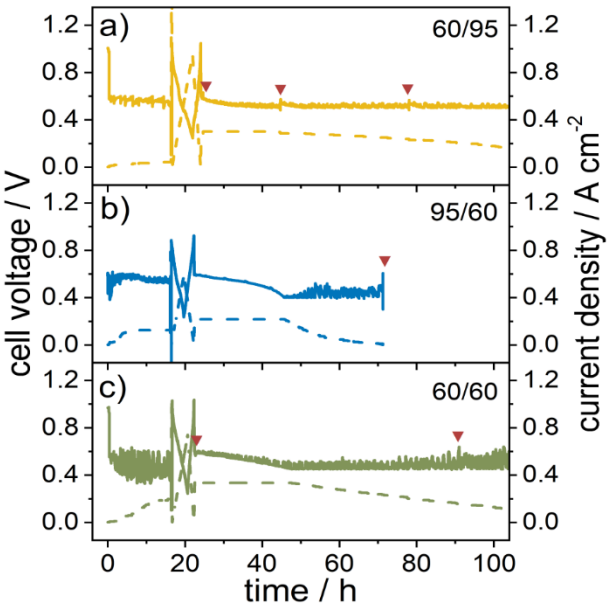

Figure 4. Performance stability of MEAs operated at different initial current densities (dashed lines) and voltage decay (solid lines) dependent on the relative humidity of the feed gases at the anode and cathode with a) 60/95 and 300 mA cm^{-2}, b) 95/60 and 216 mA cm^{-2} and c) 60/60 and 336 mA cm^{-2}. Triangles mark the points of sampling of exhaust water.

IC analysis of the exhaust water was done at several points in the course of the measurement and is provided in supporting information (Figures S6-S8), while the total loss of ionic groups after the performance stability test are shown in Figure 5. However, it should be mentioned that absolute comparability of the different MEAs is only given if exactly the same current densities and run times were applied and achieved. Due to inevitable differences between testing of MEAs and IC analysis, the interpretation of results and comparison of samples are only made qualitatively.

In case of low humidity at the anode, a total loss of 19% of ionic groups was observed, whereas the highest portion (11%) was again allocated to the polarization curves (Figure S6). Also, degradation products were mainly detected in the anode exhaust water. The initially applied current density was identical to the experiment with high RH (95/95), but the current density was

lowered after ~40 h (Figure 4a). Nevertheless, similar initial degradation rates were observed. The comparable losses of 20% (95/95) and 19% (60/95) indicate that the low RH at the anode might have an insignificant impact on the durability as lower water content might be compensated by water production of the hydrogen oxidation reaction. The lower RH at the cathode (95/60) resulted in a total loss of 15% after 70 h at an initial current density of 216 mA cm^{-2}, which had to be decreased after ~46 h to remain above the 0.4 V criteria. The fuel cell data showed a fast voltage decay with respect to the comparable low applied current density (Figure 4b), possibly indicating a degradation of the cathode ionomer and membrane as anticipated for low hydration levels at the cathode.[39] However, slightly lower amounts of degradation products were observed in IC analysis, for which the low current densities might be the reason. The MEA with low RH at both electrodes (60/60) was operated at an initial current density of 336 mA cm^{-2}, which was rapidly lowered after ~50 h due to substantial voltage decay (Figure 4c). The IC analysis resulted in 12% loss of ionic groups while slightly higher amounts of degradation products were detected after fuel cell operation (7%) compared to completion of polarization curve (5%) (Figure S8). This was not observed for the other studied samples and could be explained by slightly higher current densities (336 mA cm^{-2}) during performance stability evaluation for this case which might outweigh the degradation during the initial characterization.

Comparing the loss of ionic groups between both electrodes, in general, higher losses of degradation products were found in the samples of the anode exhaust water. Interestingly, this is not the case for low humidity at the cathode (95/60) where 9% of the loss was observed in the cathode sample. The above-described mobility of water molecules might be more limited under these conditions due to the low water gradient and hydration levels in both the membrane and the cathode (Figure S5). This is also evident from the amount of exhaust water collected in the cooling

trap of the cathode, which is even higher compared to standard conditions (95/95) and exceeds roughly six times the amount collected at the anode (cf. Tables S3 and S5). If degradation processes are more pronounced at the cathode and the membrane close to the cathode catalyst layer, the drag of degradation products was reduced for these operating conditions. But again, the observation of more degradation products at one electrode compared to the other is not necessarily caused by higher degradation rates at the anode or cathode. To further elucidate the impact of water mobility and hydration levels on observed degradation products in future studies, a water balance could be implemented by additional humidity sensors at the outlet of the cell as shown by Eriksson et al.[51] Thus, water gradients could be determined dependent on applied RH values and current densities allowing a better understanding of the transportation of degradation products across the cell. Also, *post-mortem* analysis of the individual MEA components would be necessary to further differentiate between different degradation processes.[12]

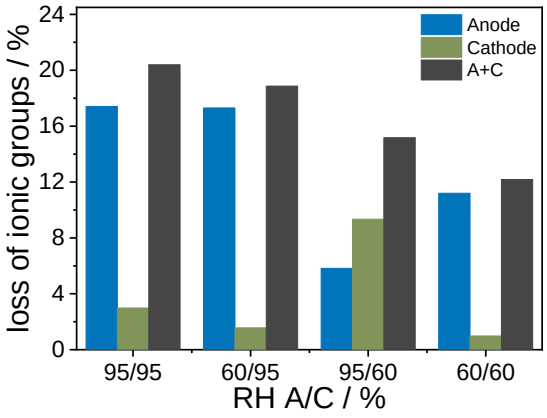

Figure 5. Loss of ionic groups during fuel cell operation dependent on the applied relative humidity of anode and cathode feed gases (A/C) quantified by ion chromatography. Data of the MEA operated at high relative humidity (95/95) are identical to Figure 2b and shown only for comparison.

The applied current densities, the achieved peak power densities as well as run times and calculated degradation rates are summarized in Table 1 in dependence on the RH. Degradation rates were calculated for the time of constant current density conditions during evaluation of the performance stability. As anticipated from the cell voltage decays, MEAs operated at RH of 95/95 and 60/95 resulted in moderate degradation rates of 4.7 mV h^{-1}. The highest rates were determined for a reduced humidity at the cathode (8.3 mV h^{-1}) and also a high rate of 5.9 mV h^{-1} was observed for reduced humidity at both electrodes. The total losses of ionic groups were highest for experiments with high humidity at both electrodes (95/95), which can be explained by longer operation at constant current density compared to the experiment with varied RH. For the MEA with low humidity at the anode (60/95) also higher amounts of degradation products were detected compared to lower humidity at the cathode or both electrodes, although the fuel cell testing resulted in lower degradation rates. This could be influenced by different applied current densities and slightly different run times as well as by the time of sampling of the exhaust water. We could demonstrate an efficient quantification and analysis of the stability of the polymer materials under different fuel cell conditions by IC analysis, although the synchronization of fuel cell data with IC investigations could be improved in the future. However, these results demonstrate the discrepancy between sufficient stability in *ex-situ* tests[34] and studies under realistic fuel cell operation; the latter confirms that a substantial improvement of the MEA longevity is necessary.[3] We believe that the application of IC will be helpful in the prospective evaluation of the performance stability and degradation pathways in the AEMFC research.

Table 1. Overview of performance and degradation data of investigated MEAs dependent on the applied relative humidity of anode and cathode feed gases.

RH at A/C [%]	Peak power density [mW cm^{-2}]	Initial applied current density @0.6 V [mA cm^{-2}]	Total run times (Time of operation at constant current density[a]) [h]	Degradation rate[b] [mV h^{-1}]	Total loss of ionic groups [%]
95/95	330	300	73 (39)	4.7	20
60/95	300	300	78 (21)	4.7	19
95/60	186	216	70 (23)	8.3	15
60/60	256	336	91 (26)	5.9	12

[a] Time of constant operation at initially applied current density before down-regulation
[b] Calculated from the cell voltage decay during time of constant operation conditions

4. Conclusion

In conclusion, the performance stability of MEAs under different fuel cell operation conditions was investigated and related to the stability of the AEM and AEI material by the IC analysis of degradation products in the exhaust water. As the main degradation product of the membrane and ionomer, carrying quaternary ammonium ions as hydroxide conducting functionality, TMA was identified based on the nucleophilic substitution as degradation pathway. For experiments at full humidity, the IC results demonstrated a high degradation, particularly after completion of begin of life characterization with equilibration and conductance of polarization curves. This provides an interesting insight into the membrane and ionomer stability under different operation conditions and reveals the necessity of choosing the characterization techniques carefully.

Furthermore, the performance stability at defined current densities was evaluated dependent on low and high RH values of the anode and cathode feed gases. Thus, low hydration levels were provoked increasing the nucleophilicity of the hydroxide ions. This leads to elevated degradation rates, which were observable in fuel cell testing. The stability decreased particularly in case of low cathode humidity which could be explained by higher sensitivity of dry-out events at the respective electrode. The degradation rates were related to the loss of functional groups determined by IC analysis, but could not be completely corelated with the detected amount of degradation products due to inevitable differences between testing of MEAs and IC analysis in this study.

In general, higher losses of ionic groups under well-humidified conditions were found in the anode exhaust water. However, this does not necessarily mean that the anode electrode is more prone to degradation. The electro-osmotic drag and the mobility of water hampers an allocation of the degradation process to a specific electrode, although some literature studies expect higher degradation rates at the cathode side especially under low humidity conditions. In consequence, higher amounts of degradation products at one electrode must not correlate with higher degradation rates at this electrode. Moreover, the degradation rates correlate not exclusively with the relative humidity, but depend also on applied current densities, run times and performed characterizations. Thus, a complex degradation behavior arises that requires further research.

In this respect, we could demonstrate the application of IC as an analytical tool in the evaluation of the stability of the AEM and AEI under fuel cell operation, which was mainly addressed in other studies by *ex-situ* studies and simulations so far. The results validate the reported dependency of the membrane durability on different humidity conditions. This initial study will guide follow-up experiments for assessing further materials and operation parameters. Especially, the influence of the begin of life characterization should be further elucidated. The application of complementing

post-mortem characterization techniques could help to differentiate between the durability of the membrane and ionomer and thus to receive a more comprehensive picture of the AEMFC longevity.

Author Information

Corresponding Author

Dr. Julian Lorenz
E-mail: julian.lorenz@dlr.de
Phone: +49-441-99906-323

Supporting Information

Supporting information: Catalyst loading of MEAs, details of IC measurements, modeling data, detailed evaluation of degradation products, loss of ionic groups for MEAs operated with varied RH.

Author Contributions

The manuscript was written through the contributions of all authors. All authors have given approval to the final version of the manuscript. ‡J.Lo. and H.J. contributed equally to this work.

Funding Sources

The authors declare no competing financial interest.

Acknowledgements

We thank Nadine Pilinski (DLR) and Vietja Tullius (DLR) for assistance in the ion chromatography measurements and fuel cell testing, respectively. This work was partly supported by the Federal Ministry of Education and Research through the project StableAPEMFC (grant number 03XP0136). J.Lo., H.J., J.Le., C.H., and A.D. thank the support by the Federal Ministry

for Economic Affairs and Climate Action as basic funding of DLR. Y.-W.C. and J.-E.C. acknowledge the research and development program of the Korea Institute of Energy Research (C0-2405). K.Y. would also like to acknowledge the financial support of the Zvi Yanai fellowship of the Ministry of Science and technology.

References

1. Wang, L.; Bellini, M.; Miller, H. A.; Varcoe, J. R., A High Conductivity Ultrathin Anion-exchange Membrane with 500+ h Alkali Stability for Use in Alkaline Membrane Fuel Cells That Can Achieve 2 W cm^{-2} at 80 °C. *J. Mater. Chem. A* **2018,** *6* (31), 15404-15412.
2. Ponce-González, J.; Varcoe, J. R.; Whelligan, D. K., Commercial Monomer Availability Leading to Missed Opportunities? Anion-Exchange Membranes Made from meta-Vinylbenzyl Chloride Exhibit an Alkali Stability Enhancement. *ACS Appl. Energy Mater.* **2018,** *1* (5), 1883-1887.
3. Dekel, D. R., Review of Cell Performance in Anion Exchange Membrane Fuel Cells. *J. Power Sources* **2018,** *375*, 158-169.
4. Huang, G.; Mandal, M.; Peng, X.; Yang-Neyerlin, A. C.; Pivovar, B. S.; Mustain, W. E.; Kohl, P. A., Composite Poly(norbornene) Anion Conducting Membranes for Achieving Durability, Water Management and High Power (3.4 W/cm^2) in Hydrogen/Oxygen Alkaline Fuel Cells. *J. Electrochem. Soc.* **2019,** *166* (10), F637-F644.
5. Adabi, H.; Shakouri, A.; Ul Hassan, N.; Varcoe, J. R.; Zulevi, B.; Serov, A.; Regalbuto, J. R.; Mustain, W. E., High-performing Commercial Fe–N–C Cathode Electrocatalyst for Anion-exchange Membrane Fuel Cells. *Nat. Energy* **2021,** *6* (8), 834-843.
6. Kabir, S.; Lemire, K.; Artyushkova, K.; Roy, A.; Odgaard, M.; Schlueter, D.; Oshchepkov, A.; Bonnefont, A.; Savinova, E.; Sabarirajan, D. C.; Mandal, P.; Crumlin, E. J.; Zenyuk, Iryna V.; Atanassov, P.; Serov, A., Platinum Group Metal-free NiMo Hydrogen Oxidation Catalysts: High Performance and Durability in Alkaline Exchange Membrane Fuel Cells. *J. Mater. Chem. A* **2017,** *5* (46), 24433-24443.
7. Yang, Y.; Peng, H.; Xiong, Y.; Li, Q.; Lu, J.; Xiao, L.; DiSalvo, F. J.; Zhuang, L.; Abruña, H. D., High-Loading Composition-Tolerant Co–Mn Spinel Oxides with Performance beyond 1 W/cm^2 in Alkaline Polymer Electrolyte Fuel Cells. *ACS Energy Lett.* **2019,** *4* (6), 1251-1257.
8. Mandal, M.; Huang, G.; Kohl, P. A., Highly Conductive Anion-Exchange Membranes Based on Cross-Linked Poly(norbornene): Vinyl Addition Polymerization. *ACS Appl. Energy Mater.* **2019,** *2* (4), 2447-2457.
9. Wright, A. G.; Fan, J.; Britton, B.; Weissbach, T.; Lee, H.-F.; Kitching, E. A.; Peckham, T. J.; Holdcroft, S., Hexamethyl-p-terphenyl poly(benzimidazolium): A Universal Hydroxide-conducting Polymer for Energy Conversion Devices. *Energy Environ. Sci.* **2016,** *9* (6), 2130-2142.

10. Varcoe, J. R.; Atanassov, P.; Dekel, D. R.; Herring, A. M.; Hickner, M. A.; Kohl, P. A.; Kucernak, A. R.; Mustain, W. E.; Nijmeijer, K.; Scott, K.; Xu, T.; Zhuang, L., Anion-exchange Membranes in Electrochemical Energy Systems. *Energy Environ. Sci.* **2014,** *7* (10), 3135-3191.
11. Gottesfeld, S.; Dekel, D. R.; Page, M.; Bae, C.; Yan, Y.; Zelenay, P.; Kim, Y. S., Anion Exchange Membrane Fuel Cells: Current Status and Remaining Challenges. *J. Power Sources* **2018,** *375*, 170-184.
12. Mustain, W. E.; Chatenet, M.; Page, M.; Kim, Y. S., Durability Challenges of Anion Exchange Membrane Fuel Cells. *Energy Environ. Sci.* **2020,** *13* (9), 2805-2838.
13. Marino, M. G.; Kreuer, K. D., Alkaline Stability of Quaternary Ammonium Cations for Alkaline Fuel Cell Membranes and Ionic Liquids. *ChemSusChem* **2015,** *8* (3), 513-523.
14. Sun, Z.; Pan, J.; Guo, J.; Yan, F., The Alkaline Stability of Anion Exchange Membrane for Fuel Cell Applications: The Effects of Alkaline Media. *Advanced Science* **2018,** *5* (8), 1800065.
15. Dekel, D. R.; Willdorf, S.; Ash, U.; Amar, M.; Pusara, S.; Dhara, S.; Srebnik, S.; Diesendruck, C. E., The Critical Relation Between Chemical Stability of Cations and Water in Anion Exchange Membrane Fuel Cells Environment. *J. Power Sources* **2018,** *375*, 351-360.
16. Sturgeon, M. R.; Macomber, C. S.; Engtrakul, C.; Long, H.; Pivovar, B. S., Hydroxide based Benzyltrimethylammonium Degradation: Quantification of Rates and Degradation Technique Development. *J. Electrochem. Soc.* **2015,** *162* (4), F366-F372.
17. Liu, L.; Chu, X.; Liao, J.; Huang, Y.; Li, Y.; Ge, Z.; Hickner, M. A.; Li, N., Tuning the Properties of Poly(2,6-dimethyl-1,4-phenylene Oxide) Anion Exchange Membranes and their Performance in H_2/O_2 Fuel Cells. *Energy Environ. Sci.* **2018,** *11* (2), 435-446.
18. Zhegur, A.; Gjineci, N.; Willdorf-Cohen, S.; Mondal, A. N.; Diesendruck, C. E.; Gavish, N.; Dekel, D. R., Changes of Anion Exchange Membrane Properties During Chemical Degradation. *ACS Appl. Polym. Mater.* **2020,** *2* (2), 360-367.
19. Hugar, K. M.; Kostalik, H. A.; Coates, G. W., Imidazolium Cations with Exceptional Alkaline Stability: A Systematic Study of Structure–Stability Relationships. *J. Am. Chem. Soc.* **2015,** *137* (27), 8730-8737.
20. Wang, L.; Brink, J. J.; Liu, Y.; Herring, A. M.; Ponce-Gonzalez, J.; Whelligan, D. K.; Varcoe, J. R., Non-fluorinated Pre-irradiation-grafted (peroxidated) LDPE-based Anion-exchange Membranes with High Performance and Stability. *Energy Environ. Sci.* **2017,** *10* (10), 2154-2167.
21. Dekel, D. R.; Amar, M.; Willdorf, S.; Kosa, M.; Dhara, S.; Diesendruck, C. E., Effect of Water on the Stability of Quaternary Ammonium Groups for Anion Exchange Membrane Fuel Cell Applications. *Chem. Mater.* **2017,** *29* (10), 4425-4431.
22. Willdorf-Cohen, S.; Mondal, A. N.; Dekel, D. R.; Diesendruck, C. E., Chemical Stability of Poly(phenylene oxide)-based Ionomers in an Anion Exchange-membrane Fuel Cell Environment. *J. Mater. Chem. A* **2018,** *6* (44), 22234-22239.
23. Dekel, D. R.; Rasin, I. G.; Brandon, S., Predicting Performance Stability of Anion Exchange Membrane Fuel Cells. *J. Power Sources* **2019,** *420*, 118-123.
24. Yassin, K.; Rasin, I. G.; Brandon, S.; Dekel, D. R., Quantifying the Critical Effect of Water Diffusivity in Anion Exchange Membranes for Fuel Cell Applications. *J. Membr. Sci.* **2020,** *608*, 118206.
25. Bharath, V. J.; Millichamp, J.; Neville, T. P.; Mason, T. J.; Shearing, P. R.; Brown, R. J. C.; Manos, G.; Brett, D. J. L., Measurement of Water Uptake in Thin-film Nafion and Anion Alkaline Exchange Membranes Using the Quartz Crystal Microbalance. *J. Membr. Sci.* **2016,** *497*, 229-238.

26. Kreuer, K.-D.; Jannasch, P., A Practical Method for Measuring the Ion Exchange Capacity Decrease of Hydroxide Exchange Membranes During Intrinsic Degradation. *J. Power Sources* **2018,** *375*, 361-366.
27. Gao, X.; Yu, H.; Jia, J.; Hao, J.; Xie, F.; Chi, J.; Qin, B.; Fu, L.; Song, W.; Shao, Z., High Performance Anion Exchange Ionomer for Anion Exchange Membrane Fuel Cells. *RSC Advances* **2017,** *7* (31), 19153-19161.
28. Zeng, L.; Zhao, T. S.; An, L., A High-performance Supportless Silver Nanowire Catalyst for Anion Exchange Membrane Fuel Cells. *J. Mater. Chem. A* **2015,** *3* (4), 1410-1416.
29. Lu, W.; Shao, Z.-G.; Zhang, G.; Zhao, Y.; Yi, B., Crosslinked Poly(vinylbenzyl chloride) with a Macromolecular Crosslinker for Anion Exchange Membrane Fuel Cells. *J. Power Sources* **2014,** *248*, 905-914.
30. Peng, X.; Kulkarni, D.; Huang, Y.; Omasta, T. J.; Ng, B.; Zheng, Y.; Wang, L.; LaManna, J. M.; Hussey, D. S.; Varcoe, J. R.; Zenyuk, I. V.; Mustain, W. E., Using Operando Techniques to Understand and Design High Performance and Stable Alkaline Membrane Fuel Cells. *Nat. Commun.* **2020,** *11* (1), 3561.
31. Ul Hassan, N.; Mandal, M.; Huang, G.; Firouzjaie, H. A.; Kohl, P. A.; Mustain, W. E., Achieving High-Performance and 2000 h Stability in Anion Exchange Membrane Fuel Cells by Manipulating Ionomer Properties and Electrode Optimization. *Adv. Energy Mater.* **2020,** *10* (40), 2001986.
32. Maurya, S.; Lee, A. S.; Li, D.; Park, E. J.; Leonard, D. P.; Noh, S.; Bae, C.; Kim, Y. S., On the Origin of Permanent Performance Loss of Anion Exchange Membrane Fuel Cells: Electrochemical Oxidation of Phenyl Group. *J. Power Sources* **2019,** *436*, 226866.
33. Matanovic, I.; Chung, H. T.; Kim, Y. S., Benzene Adsorption: A Significant Inhibitor for the Hydrogen Oxidation Reaction in Alkaline Conditions. *J. Phys. Chem. Lett.* **2017,** *8* (19), 4918-4924.
34. Lee, M.-S.; Kim, T.; Park, S.-H.; Kim, C.-S.; Choi, Y.-W., A Highly Durable Cross-linked Hydroxide Ion Conducting Pore-filling Membrane. *J. Mater. Chem.* **2012,** *22* (28), 13928-13931.
35. Oda, K.; Kato, H.; Fukuta, K.; Yanagi, H., Optimization of RRDE Method for the Evaluation of Catalyst Activity in Alkaline Solution. *ECS Meeting Abstracts* **2010,** *MA2010-01* (3), 192-192.
36. Omasta, T. J.; Wang, L.; Peng, X.; Lewis, C. A.; Varcoe, J. R.; Mustain, W. E., Importance of Balancing Membrane and Electrode Water in Anion Exchange Membrane Fuel Cells. *J. Power Sources* **2018,** *375* (Supplement C), 205-213.
37. Isomura, T., AMFC Activity in Tokuyama Corporation. In *Workshop on Ion Exchange Membranes for Energy Applications – EMEA2016*, Bad Zwischenahn, Germany, 2016; p 28.
38. Metrohm *Methylamines and Ethanolamines (Metrosep C 4 - 150)*; IC Application Note No. C-126.
39. Dekel, D. R.; Rasin, I. G.; Page, M.; Brandon, S., Steady State and Transient Simulation of Anion Exchange Membrane Fuel Cells. *J. Power Sources* **2018,** *375*, 191-204.
40. Adabi, H.; Santori, P. G.; Shakouri, A.; Peng, X.; Yassin, K.; Rasin, I. G.; Brandon, S.; Dekel, D. R.; Hassan, N. U.; Sougrati, M.-T.; Zitolo, A.; Varcoe, J. R.; Regalbuto, J. R.; Jaouen, F.; Mustain, W. E., Understanding How Single-atom Site Density Drives the Performance and Durability of PGM-free Fe–N–C Cathodes in Anion Exchange Membrane Fuel Cells. *Mater. Today Adv.* **2021,** *12*, 100179.

41. Reshetenko, T.; Odgaard, M.; Schlueter, D.; Serov, A., Analysis of Alkaline Exchange Membrane Fuel Cells Performance at Different Operating Conditions using DC and AC Methods. *J. Power Sources* **2018,** *375* (Supplement C), 185-190.
42. Omasta, T. J.; Park, A. M.; LaManna, J. M.; Zhang, Y.; Peng, X.; Wang, L.; Jacobson, D. L.; Varcoe, J. R.; Hussey, D. S.; Pivovar, B. S.; Mustain, W. E., Beyond Catalysis and Membranes: Visualizing and Solving the Challenge of Electrode Water Accumulation and Flooding in AEMFCs. *Energy Environ. Sci.* **2018,** *11* (3), 551-558.
43. Kaspar, R. B.; Letterio, M. P.; Wittkopf, J. A.; Gong, K.; Gu, S.; Yan, Y., Manipulating Water in High-Performance Hydroxide Exchange Membrane Fuel Cells through Asymmetric Humidification and Wetproofing. *J. Electrochem. Soc.* **2015,** *162* (6), F483-F488.
44. Deng, H.; Wang, D.; Wang, R.; Xie, X.; Yin, Y.; Du, Q.; Jiao, K., Effect of Electrode Design and Operating Condition on Performance of Hydrogen Alkaline Membrane Fuel Cell. *Appl. Energ.* **2016,** *183*, 1272-1278.
45. Carmo, M.; Doubek, G.; Sekol, R. C.; Linardi, M.; Taylor, A. D., Development and Electrochemical Studies of Membrane Electrode Assemblies for Polymer Electrolyte Alkaline Fuel Cells Using FAA Membrane and Ionomer. *J. Power Sources* **2013,** *230*, 169-175.
46. Yanagi, H.; Fukuta, K. In *Anion Exchange Membrane and Ionomer for Alkaline Membrane Fuel Cells (AMFCs)*, ECS Trans., Honolulu, HI, Honolulu, HI, 2008; pp 257-262.
47. Diesendruck, C. E.; Dekel, D. R., Water – A Key Parameter in the Stability of Anion Exchange Membrane Fuel Cells. *Curr. Opin. Electrochem.* **2018,** *9*, 173-178.
48. Schonvogel, D.; Rastedt, M.; Wagner, P.; Wark, M.; Dyck, A., Impact of Accelerated Stress Tests on High Temperature PEMFC Degradation. *Fuel Cells* **2016,** *16* (4), 480-489.
49. Yassin, K.; Rasin, I. G.; Brandon, S.; Dekel, D. R., Elucidating the Role of Anion-exchange Ionomer Conductivity within the Cathode Catalytic Layer of Anion-exchange Membrane Fuel Cells. *J. Power Sources* **2022,** *524*, 231083.
50. Yassin, K.; Rasin, I. G.; Willdorf-Cohen, S.; Diesendruck, C. E.; Brandon, S.; Dekel, D. R., A Surprising Relation Between Operating Temperature and Stability of Anion Exchange Membrane Fuel Cells. *J. Power Sources Adv.* **2021,** *11*, 100066.
51. Eriksson, B.; Grimler, H.; Carlson, A.; Ekström, H.; Wreland Lindström, R.; Lindbergh, G.; Lagergren, C., Quantifying Water Transport in Anion Exchange Membrane Fuel Cells. *Int. J. Hydrogen Energy* **2019,** *44* (10), 4930-4939.

Table of Content Graphic